

# Three-Dimensional Simulation of Stokes Flow Around a Rigid Structure Using FMM/GPU Accelerated BEM

Olga A. Abramova<sup>1</sup> ✉, Yulia A. Pityuk<sup>1</sup>, Nail A. Gumerov<sup>1,2</sup>, and  
Iskander Sh. Akhatov<sup>3</sup>

<sup>1</sup> Center for Micro and Nanoscale Dynamics of Dispersed Systems,  
Bashkir State University, Ufa, Russia

<sup>2</sup> Institute for Advanced Computer Studies,  
University of Maryland, USA

<sup>3</sup> Skolkovo Institute of Science and Engineering (Skoltech), Russia.  
abramovacmdds@gmail.com

**Abstract.** Composite materials play an important role in aircraft, space and automotive industries, wind power industry. One of the most commonly used methods for the manufacture of composite materials is the impregnation of dry textiles by a viscous liquid binder. During the process, cavities (voids) of various sizes can be formed and then move in a liquid resin flows in the complex system of channels formed by textile fibers. The presence of such cavities results in a substantial deterioration of the mechanical properties of the composites. As a result, the development and effective implementation of the numerical methods and approaches for the effective 3D simulation of the viscous liquid flow around a rigid structure of different configuration. In the present study, the mathematical model and its effective numerical implementation for the study of hydrodynamic processes around fixed structure at low Reynolds numbers is considered. The developed approach is based on the boundary element method for 3D problems accelerated both via an advanced scalable algorithm (FMM), and via utilization of a heterogeneous computing architecture (multicore CPUs and graphics processors). This enables direct large scale simulations on a personal workstation, which is confirmed by test and demo computations. The simulation results and details of the method and accuracy/performance of the algorithm are discussed. The results of the research may be used for the solution of problems related to microfluidic device construction, theory of the composite materials production, and are of interest for computational hydrodynamics as a whole.

**Keywords:** Stokes Flow · Boundary Element Method · Fast Multipole Method · High-Performance Computing · GPUs

## 1 Introduction

Composite materials are man-made combinations of two or more different materials that produce new materials having unique properties, such as improved

stiffness, or tailored thermal or electrical conductivity. A main driver for the development of composites has been the increasing need for materials that are at the same time stiff and light, to be used in aircraft, space industries. Other rapidly expanding fields of applications encompass energy generation (wind energy notably), infrastructure and architecture (bridges and buildings), transportation including automotive, marine and rail, as well as biomedical engineering. One of the most commonly used methods for the manufacture of composite materials is the impregnation of dry textiles by a viscous liquid binder. During the impregnation, a liquid resin flows in the complex system of channels formed by textile fibers, which can be considered as a porous medium. In the process of filling the reinforcing structure by the liquid, cavities (voids) of various sizes can be formed. The presence of voids significantly reduces the mechanical properties of composites and increasing design risk. Therefore, the reduction of void content is critical. A common point of view is that the formation of such voids is due to the heterogeneity of the porous structure, which for textiles has two characteristic scales. The microscale is associated with a diameter and packing of individual fibers in the filament, while the mesoscale is associated with a location of filaments in the structure of the reinforcing fabric and with a distance between the layers in multilayer structures. Currently, there are proven algorithms for solving problems of the composites impregnation at the macro level that allows us to describe the overall picture of filling of the preform by binder. Methods of simulation of the impregnation that are based on the solution of the Darcy's equation and given local permeability of the medium are well known and formalized in software packages, that are widely used in research organizations and industry for the design of the impregnation process. However, these methods do not allow to predict the voids volume fraction, their size and shape, since the voids formation is due to the physics of the processes on a smaller scale and cannot be described by Darcy's law. Wide range of work is dedicated to the experimental [10, 5] and numerical [16, 4, 20, 6, 15] studying of the processes, which associated with the complicated flows that occur while liquid composite moulding (LCM). Since manufacturing of a composite part is in general performed by infiltration of the liquid matrix into the thin porous medium made from the fibre assembly, the direct three-dimensional numerical simulation of viscous liquid flow around the complicated structure is of interest. Nowadays, modern computational methods and powerful computer resources enable fast large-scale microfluid dynamics simulations, which makes them a valuable research tool. The present work is devoted to the application of efficient computational techniques for the 3D modeling of viscous fluid flow in complex domains containing rigid structures, corresponding to filaments assembly, at low Reynolds numbers. The numerical approach is based on the boundary element method (BEM) accelerated both via advanced scalable algorithms, particularly, the fast multipole method (FMM), and via utilization of advanced hardware, particularly, graphics processors (GPUs) and multicore CPUs. This technique we developed and applied for research the 3D emulsion dynamics and viscous fluid flow in various domains [1–3] and bubble dynamics at low [13] and moderate [14] Reynolds

numbers. In our previous works example computations were successfully conducted for 3D dynamics of systems of tens of thousands of deformable drops and systems of several droplets, with very high discretization of the interface in a shear flow [1].

The BEM has been successfully applied for simulation of Stokes flows ([23]; see general overview and details of the BEM in the monograph of Pozrikidis [17]), but its application to simulation of large non-periodic systems is very limited. Thus, the key here is the application of fast algorithms for BEM acceleration. The FMM was first introduced by Rokhlin and Greengard [7] as a method for fast summation of electrostatic or gravitational potentials in two and three dimensions. The first application of the FMM for the solution of Stokes equations in the case of spherical rigid particles was reported by Sangani and Mo [19]. In the work [22], the authors achieved substantial accelerations of droplet dynamics simulations via the use of multipole expansions and translation operators, which is very much in the spirit of the FMM, and can be considered as one- and two-level FMM. However, the  $O(N)$  scalability of the FMM can be achieved only on hierarchical (multilevel) data structures, which were not implemented there. Note that the FMM can be efficiently parallelized. The first implementation of the FMM on graphics processors was reported by Gumerov and Duraiswami [8], who showed that the use of a GPU for the FMM for the Laplace's equation in 3D can produce 30 to 60-fold accelerations, and achieved a time of 1 second for the MVP in a case of size 1 million on a single GPU. This approach was developed further and papers by Hu *et al.* [11, 12] present scalable FMM algorithms and implementations of heterogeneous computing architectures that may contain many distributed nodes, each of them consisting of one multicore CPU and several GPUs. They performed the MVP for a system of size 1 billion achieving a time of about 10 seconds on a 32-node cluster, and also for systems of size 1 million in a time of the order of several tenths of a second on a single heterogeneous CPU/GPU node. In the present study, we use a single heterogeneous node with one GPU and apply CPU/GPU parallelism. This realization enables computations of 3D fluid flow at low Reynolds numbers around the structures complicated configurations with tens of thousands triangular elements discretizing the boundary.

## 2 Problem Statement

In this paper, we consider the viscous fluid flow around a non-deformable fixed object in Cartesian coordinates. It is assumed that the processes are isothermal and slowly enough that the viscosity forces are much more significant than the inertia forces. In this case, the steady flow of incompressible liquids is described by the Stokes equations [9] (1) with the corresponding boundary conditions (2).

$$\nabla \cdot \boldsymbol{\sigma} = -\nabla p + \mu \nabla^2 \mathbf{u} = \mathbf{0}, \quad \nabla \cdot \mathbf{u} = 0, \quad (1)$$

where  $\mathbf{u}$  and  $\boldsymbol{\sigma}$  are the velocity and the stress tensors,  $\mu$  is the dynamic viscosity, and  $p$  is the pressure, which includes the hydrostatic component.

4 3D Simulation of Stokes Flow Using FMM/GPU Accelerated BEM

At the surface of non-deformable fixed structures  $S$

$$\mathbf{u}(\mathbf{x}) = 0, \quad \mathbf{x} \in S, \quad (2)$$

where  $\mathbf{x}$  is the radius vector of the current point.

For the carrier fluid the condition  $\mathbf{u}(\mathbf{x}) \rightarrow \mathbf{u}_\infty(\mathbf{x})$  is imposed, where  $\mathbf{u}_\infty(\mathbf{x})$  is a solution of the Stokes equations.

### 3 Numerical Implementation

The problem is solved using the boundary element method, which is based on the integral equations for the determination of the velocity distribution over the boundary. There is no need to cover all computational domain by mesh as in the case of finite-difference and finite-element methods, but only the boundary of the considered objects. As a result, the BEM is very efficient for solving 3D problems with complicated geometries or in infinite domains.

The boundary integral equations for the volume of fluid occupying domain  $V$  bounded by surface  $S$  can be written in the form [17]

$$\begin{aligned} \mathbf{u}(\mathbf{y}) - \int_S \mathbf{K}(\mathbf{y}, \mathbf{x}) \cdot \mathbf{u}(\mathbf{x}) dS(\mathbf{x}) &= \frac{1}{\mu} \int_S \mathbf{G}(\mathbf{y}, \mathbf{x}) \cdot \mathbf{f}(\mathbf{x}) dS(\mathbf{x}), \quad \mathbf{y} \in V, \\ \frac{1}{2} \mathbf{u}(\mathbf{y}) - \int_S \mathbf{K}(\mathbf{y}, \mathbf{x}) \cdot \mathbf{u}(\mathbf{x}) dS(\mathbf{x}) &= \frac{1}{\mu} \int_S \mathbf{G}(\mathbf{y}, \mathbf{x}) \cdot \mathbf{f}(\mathbf{x}) dS(\mathbf{x}), \quad \mathbf{y} \in S, \\ - \int_S \mathbf{K}(\mathbf{y}, \mathbf{x}) \cdot \mathbf{u}(\mathbf{x}) dS(\mathbf{x}) &= \frac{1}{\mu} \int_S \mathbf{G}(\mathbf{y}, \mathbf{x}) \cdot \mathbf{f}(\mathbf{x}) dS(\mathbf{x}), \quad \mathbf{y} \notin S, V, \end{aligned} \quad (3)$$

where the fundamental solutions (Stokeslet and stresslet) are given by the second and third rank tensors

$$\begin{aligned} \mathbf{G}(\mathbf{y}, \mathbf{x}) &= \frac{1}{8\pi} \left( \frac{\mathbf{I}}{r} + \frac{\mathbf{r}\mathbf{r}}{r^3} \right), \quad \mathbf{T}(\mathbf{y}, \mathbf{x}) = -\frac{3}{4\pi} \frac{\mathbf{r}\mathbf{r}\mathbf{r}}{r^5}, \\ \mathbf{K}(\mathbf{y}, \mathbf{x}) &= \mathbf{T}(\mathbf{y}, \mathbf{x}) \cdot \mathbf{n}(\mathbf{x}), \quad \mathbf{r} = \mathbf{y} - \mathbf{x}, \quad r = |\mathbf{r}|, \end{aligned} \quad (4)$$

and  $\mathbf{I}$  is the identity tensor,  $\mathbf{n}$  is the normal to  $S$ . Thus, if  $\mathbf{u}$  and  $\mathbf{f}$  are known on the boundaries, the velocity field  $\mathbf{u}(\mathbf{y})$  can be determined at the any spatial point.

The problem describes a flow around the structures in an unbounded domain. In this case,  $\mathbf{u}_\infty$  is prescribed (e.g., a uniform constant flow  $\mathbf{u}_\infty = (U, 0, 0)$ ), and the boundary integral equation (3) with taking into account the boundary conditions (2) and that the normal pointed into fluid, can be written in the form

$$\left. \begin{aligned} \mathbf{y} \in V, \quad \mathbf{u}(\mathbf{y}) - 2 \cdot \mathbf{u}_\infty(\mathbf{y}) \\ \mathbf{y} \in S, \quad \frac{1}{2} \mathbf{u}(\mathbf{y}) - \mathbf{u}_\infty(\mathbf{y}) \end{aligned} \right\} = \int_S \left\{ -\frac{1}{\mu} \mathbf{G}(\mathbf{y}, \mathbf{x}) \cdot \mathbf{f}(\mathbf{x}) \right\} dS(\mathbf{x}). \quad (5)$$

The numerical method is based on the discretization of object surfaces by triangular meshes. The regular integrals over the patches were computed using

second order accuracy formulae (trapezoidal rules). The collocation points for a rigid structure surface were located at the center of triangular elements. The computation of singular integrals was performed based on the integral identities for the Stokeslet and stresslet integrals (see [17, 23]), which allow to express these integrals via sums of regular integrals over the rest of the surface. More details of the present implementation can be found in [1, 2].

The boundary integral equations combined with the boundary conditions in discrete form result in a system of linear algebraic equations (SLAE)

$$\mathbf{A}\mathbf{X} = \mathbf{b}, \quad (6)$$

where  $\mathbf{A}$  is the system matrix,  $\mathbf{X}$  is the solution vector, and  $\mathbf{b}$  is the right-hand-side vector.

#### 4 Acceleration of Calculations

Numerical modeling of 3D Stokes flows in regions of non-trivial geometry is a computationally complex and resource-intensive process. Note that calculations using a standard BEM take significant time even for a relatively small mesh resolution of the object surfaces. This is due to the fact that BEM reduces to solving a dense SLAE concerning  $3N$  of unknowns (6). Furthermore, the memory required for computations increases proportionally to the square of the number of mesh points. Solving such a large problem requires development and application of efficient numerical methods and techniques.

The direct methods of solution of algebraic systems, having computational complexity  $O(N^3)$ , become impractical when  $N$  reaches a value of the order of millions. The use of efficient iterative methods reduces this complexity to  $O(N_{\text{iter}}N^2)$ , where  $N_{\text{iter}} \ll N$  is the number of iterations, and  $O(N^2)$  is the cost of a single matrix-vector product (MVP). In this paper, we used the unpreconditioned general minimal residual method (GMRES) to solve the system [18]. The main computational complexity of the problem is in the calculation of MVP at each iteration. That is why in this study the program module of MVP is accelerated in order to implement the iterative method effectively. Acceleration of MVP is possible due to: 1) application of modern highly efficient methods and algorithms to reduce computational complexity; 2) using of high-performance hardware.

First, in order to speedup the calculations and increasing the problem size we developed program code for MVP without matrix storage in the memory of computational system (“MV Product on the fly”). Each element of matrices  $\mathbf{G}$  is calculated using the formulas (4). This program was implemented on GPUs using CUDA technology. Performing calculations on the graphics processors shows excellent results in algorithms that involve parallel processing of data (applying the same sequence of mathematical operations to a set of data), that is why we use GPUs in our study. Herewith the best results are achieved if the ratio of the number of arithmetic instructions to the number of accesses to memory is large enough. The parallelization of the module “MV Product on the fly” is based

on the partitioning of the matrices by horizontal bands into  $m$  parts such that  $M = m \times L$ , where  $M$  is the dimension of the matrix,  $L$  is the number of rows of the matrix in the block,  $m$  is the number of threads on the GPUs. At each iteration, each of the  $m$  threads computes its part of the solution vector. Each thread stores a part of the resulting vector in the local memory, which is copied to the global memory at the end of the calculation to obtain a complete solution vector.

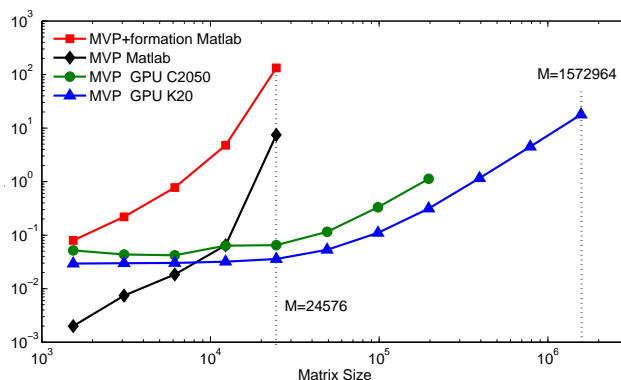


Fig. 1. Runtime for MVP module

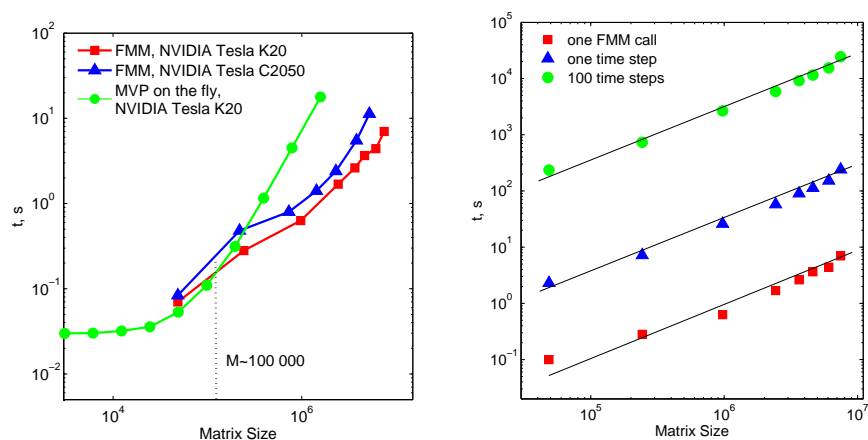
The tests were performed on workstations of two configurations: 1) CPU Intel Xeon 5660 and GPUs NVIDIA Tesla K20, 5 GB of global memory (Kepler architecture); 2) CPU Intel Xeon 5660 and GPUs NVIDIA Tesla C2050, 3 GB of global memory (Fermi architecture).

Fig. 1 shows a comparison of the MVP execution time on the GPUs and the built-in Matlab function including (MVP + formation) and without (Matlab MVP) matrix formation depending on matrix size ( $M = 3 \cdot N$ ). It can be seen from the curves that starting with a relatively small  $M \approx 2.5 \cdot 10^4$  there is a shortage of the memory of the computer system and further calculations becomes impossible. However the module implemented on the GPUs allows one to solve problems of larger computational complexity. Numerical experiments on the NVIDIA Tesla K20 show the possibility of solving boundary problems for Stokes equations up to  $3 \cdot 10^5$  calculation points on one personal workstation in a reasonable time.

But for larger  $N$ , this is not fast enough even when using high-performance computing, since the computational cost increases proportionally to the square of  $N$ . Thus, the key here is that the MVP specific for the present problem can be computed using the FMM [7]. The main advantage of this method is that the complexity of the MVP involving a certain type of dense matrices can be reduced from  $O(N^2)$  to  $O(N \log(N))$ , or even  $O(N)$ . In this paper, we used the implementation technique of the FMM for the summation of the Stokeslets and stresslets (Eq. (4)) proposed in [21]. This approach is based on the summation of the fundamental solutions of the three-dimensional Laplace's equation. In the

3D Simulation of Stokes Flow Using FMM/GPU Accelerated BEM

7



(a) The runtime of the MVP module and (b) The wall-clock time on the PC with FMM routine NVIDIA Tesla K20 [1]

**Fig. 2.** Runtime for MVP of different implementations

present approach, GPUs acceleration is used in the so-called heterogeneous FMM algorithm, where the system matrix can be decomposed as sum of the two parts: dense and sparse. Subroutines for dense part produce approximate dense MVP on the CPU using OpenMP, and subroutines for sparse part produce direct sparse multiplication on the GPUs using CUDA. A careful tuning of the algorithm and the data structure octree depth is based on the work load balance between the CPU and GPUs. Using such an heterogeneous algorithm on a system with 8 to 12 CPU cores and one GPUs, the overall acceleration can rise by approximately 100 times compared to its value for a single-core CPU implementation. The features of the algorithm and implementations are presented in [2, 8].

It is seen from the Fig. 2(left) that starting with a certain size of the matrix  $M \approx 1 \cdot 10^5$  the using of heterogeneous FMM is preferable for numerical experiments. Numerical experiments show (Fig. 1,2) that the calculations on the NVIDIA Tesla K20 graphics card with the Kepler architecture take less time than ones on the NVIDIA Tesla C2050 GPUs with the Fermi architecture, for any matrix size. In Fig. 2(right), the computational wall-clock times for one FMM call, for one time step and for one hundred time steps are shown as functions of the matrix size. In our work [1] it was reported that the run time for one FMM call for the system with  $M \approx 7.5 \cdot 10^6$  was about 7 seconds; for one time step, it was 4 minutes, and for 100 time steps, about 7 hours on one personal workstation. It can be seen that these functions are close to linear. This allows one to estimate the computational times for larger scale problems. The use of the FMM for MVP reduces the computational complexity of the overall prob-

8 3D Simulation of Stokes Flow Using FMM/GPU Accelerated BEM

lem to  $O(N_{\text{iter}}N)$  per time step, and potentially can handle direct large scale simulations with millions of boundary elements.

### 5 Numerical Results and Discussion

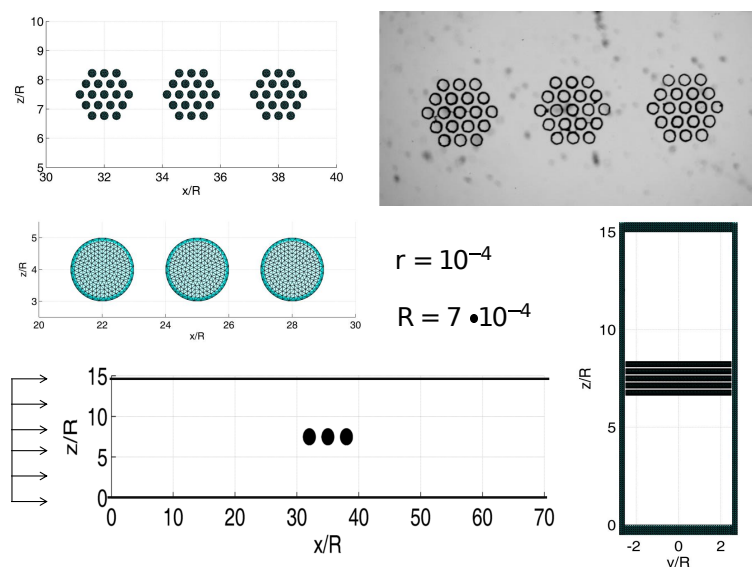
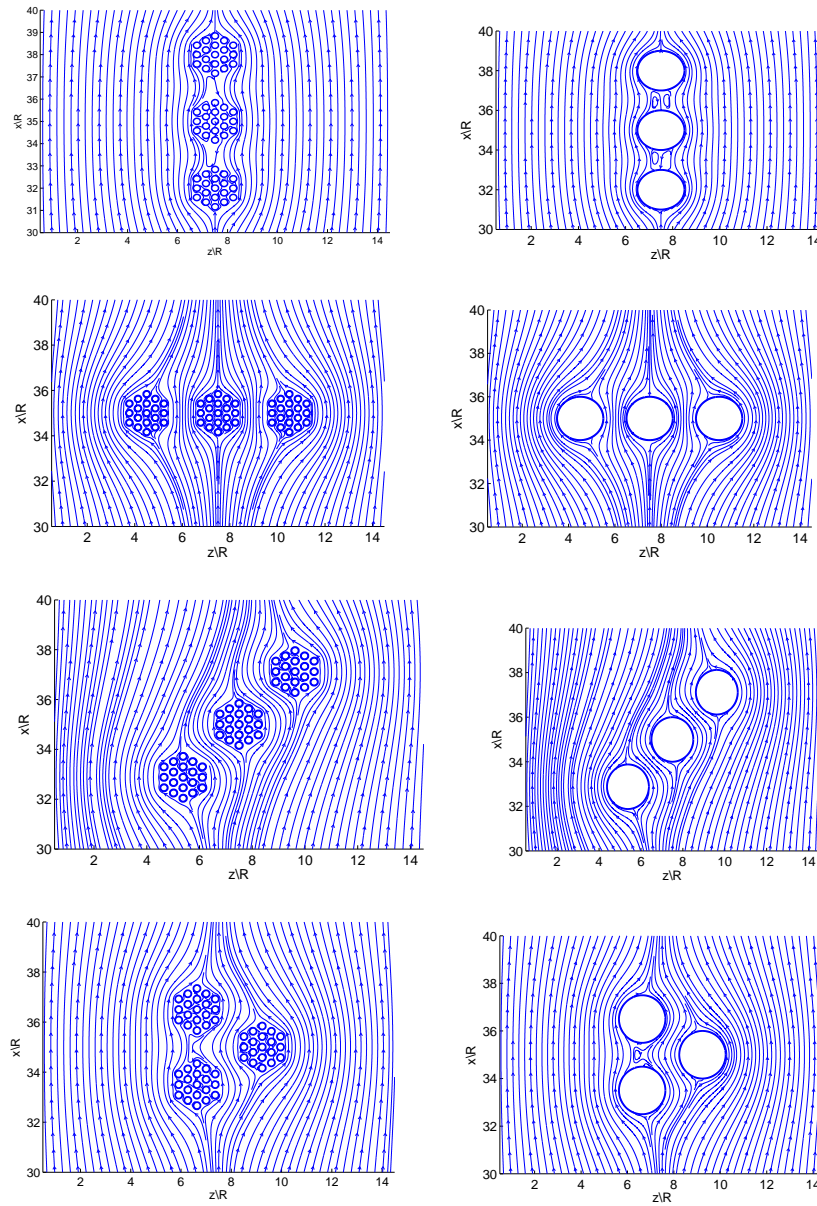


Fig. 3. Geometry of the considered domain

Numerical tests are performed on a workstation equipped with two Intel Xeon 5660, and one NVIDIA Tesla K20. Several algorithm implementations were done, including CPU and CPU/GPUs versions of the iterative algorithm with the FMM accelerated MVP and a conventional BEM in which the BEM matrices were computed and stored. The latter implementation was developed for verification and validation purposes to ensure that the algorithms produce consistent results.

The implemented methods were tested for the case of one fixed rigid sphere in an unbounded flow. The obtained results were compared against the analytical solution [9]. The relative error in the  $L_\infty$ -norm was 0.08 – 0.1% for the velocity component around the sphere, and for traction on the sphere surface the relative error was about 1.8%, for  $N_\Delta = 1380$  triangular elements on the surface. The error decreases as the number of mesh points increases.

We conducted simulations of the viscous fluid flow around the fixed rigid structures formed by cylindrical elements with a radius  $R$  by an infinite flow with the constant velocity  $\mathbf{u}_\infty(\mathbf{x}) = (U, 0, 0)$  at infinity. Represented numerical



**Fig. 4.** Streamlines around the assembly of filaments,  $Re = 0.5$ .

research are motivated by the study of processes occurring while the viscous binding fluid flow around reinforcement fibers in the manufacture of composite materials. Further comparison of the simulation results of the flow pattern will

be carried out with experimental data that will be obtained in the experimental laboratory of our Center. A series of experiments is planned to study the flow pattern around individual filaments and assembly of filaments. Several microdevices are already made for the study of flows in samples with double porosity (Fig. 3, right top corner).

The geometry used in the computational examples for simulation of the single and double porosity is shown in Fig.3. Structure of the filaments is bounded by the flat planes, which geometry characteristics correspond to the experimental data:  $L_x \gg R$ ,  $L_y = 5 \cdot R$ ,  $L_z = 5 \cdot R$ . In the case of single porosity there was three individual fibers of radius  $R$  and the surface of each cylindrical element was covered by mesh with  $N_{\Delta} = 2920$  triangular elements, on the surface of each flat plane summary was  $N_{\Delta} = 234200$ . As a result the problem size and matrix size were  $N = 242960$  and  $M = 728880$  respectively. Since the problem size is moderate, the calculations were carried out by BEM accelerated only due to the MVP routine at the GPUs. As for the double porosity, the structure consists of 57 cylindrical elements of the same radius  $r = \frac{1}{7}R$  with  $N_{\Delta} = 2504$  on each surface, on the surface of all flat plane summary was  $N_{\Delta} = 886400$ . Thus, the total number of computational points in this case was  $N = 1029128$ . Note that this leads to the solution of a linear system with  $\sim 3.5 \cdot 10^6$  independent variables. In this case the using of FMM accelerated BEM is preferable.

Fig. 4 shows the calculation results of the components of the velocity field around the fixed rigid filaments in different configurations for the cases of single (Fig. 4 on the right) and double (Fig. 4 on the left) porosity, at  $Re = 0.5$ , fragment of the computational domain  $30 \cdot R \leq x \leq 40 \cdot R$ ,  $0.5 \cdot R \leq z \leq 14.5 \cdot R$  in the plane  $y = 0$ . The distance between assembly of filaments was  $R$  and between the individual small filaments was  $r$ . It is seen that double porosity influence on the flow pattern between the filaments. Further, the results of the studies will be compared with the experimental data. In addition, flow patterns can be useful in studying the dynamics of voids during the impregnation of reinforcing structures.

## 6 Conclusions

The problem statement for steady viscous fluid flow around the fixed rigid structures is developed and implemented. The numerical approach is based on the boundary element method for three-dimensional problems accelerated by utilization of a graphics processors using CUDA technology and via an advanced scalable heterogeneous algorithm (FMM). The program modules are tested on workstations with GPUs of different architectures, the performance is studied and the optimal parameters are chosen. The software implementation allows to select an appropriate algorithms for MVP calculation depending on the problem size. The verification and validation of the developed codes showed that the algorithms produce consistent results. The paper presents the results of modeling of 3D Stokes flow of a viscous fluid in a complex geometry, corresponding to the fibrous reinforcement of composite materials. Nevertheless the cases considered

in the present work require more detailed studies for understanding the factors that affect the flow patterns. The results showed that the developed software enables direct flow simulations in the structures with interfaces discretized by millions of boundary elements on personal supercomputers. The presented algorithms can be mapped onto heterogeneous computing clusters [12], which should both accelerate computations and allow for the treatment of larger systems. The developed software can become a valuable research tool for investigation the influence of geometry features of the reinforcing structure on the flow of viscous liquid and liquid with bubbles to study the formation and dynamics of voids during the manufacturing of composite materials.

## Acknowledgements

This study is supported in part by the Skoltech Partnership Program (developing and testing of the accelerated BEM version, conducting of the calculations), part of the study devoted to the problem formulation of the flow near rigid structures is carried out with the support of the grant RFBR 18-31-00074, and FMM routine is provided by Fantalgo, LLC (Maryland, USA).

## References

1. Abramova, O.A., Pityuk, Yu.A., Gumerov, N.A., Akhatov, I. Sh. High performance BEM simulation of 3D emulsion flow. Communications in Computer and Information Science (CCIS). V 753. pp. 317-330 (2017). [https://doi.org/10.1007/978-3-319-67035-5\\_23](https://doi.org/10.1007/978-3-319-67035-5_23)
2. Abramova, O.A., Itkulova, Yu.A., Gumerov, N.A., Akhatov, I.Sh. Three-dimensional simulation of the dynamics of deformable droplets of an emulsion using the boundary element method and the fast multipole method on heterogeneous computing systems. Vychislitelnye Metody i Programirovanie. 14, pp. 438-450 (2013)
3. Abramova O.A., Itkulova Yu.A., Gumerov N.A. FMM/GPU Accelerated BEM Simulations of Emulsion Flows in Microchannels. Contribution paper of ASME 2013 IMECE. (2013). <https://doi.org/10.1115/imece2013-63193>
4. Arcila, I.P., Power, H., Londono, C.N., Escobar, W.F. Boundary Element Method for the dynamic evolution of intra-tow voids in dual-scale fibrous reinforcements using a Stokes-Darcy formulation. Eng Analysis with Boundary Elements. vol. 87. pp. 133-152 (2018). <https://doi.org/10.1017/s0022112069000759>
5. Gangloff Jr., J.J., Daniel, C., Advani, S.G. A model of a two-phase resin and void flow during composites processing. Int. J. Multiphase Flow. vol. 65. pp. 51-60 (2014). <https://doi.org/10.1016/j.ijmultiphaseflow.2014.05.015>
6. Gascon L., Garcia J.A., Lebel F., Ruiz E. and Trochu F. Numerical prediction of saturation in dual scale fibrous reinforcements during Liquid Composite Molding. Composites Part a-Applied Science and Manufacturing. vol. 77. pp. 275-284. (2015) <https://doi.org/10.1016/j.compositesa.2015.05.019>
7. Greengard, L., Rokhlin, V. A fast algorithm for particle simulations. J. Comp. Phys. vol. 73, pp. 325-348 (1987) <https://doi.org/10.1006/jcph.1997.5706>

12 3D Simulation of Stokes Flow Using FMM/GPU Accelerated BEM

8. Gumerov, N.A., Duraiswami, R. Fast multipole methods on graphics processors. *J. Comput. Phys.* vol. 227(18), pp. 8290-8313 (2008) <https://doi.org/10.1016/j.jcp.2008.05.023>
9. Happel, J., Brenner, H. *Low Reynolds number hydrodynamics*. Springer Netherlands. p. 553 (1981) <https://doi.org/10.1007/978-94-009-8352-6>
10. Hamidi, Y. K., Aktas, L., Altan, M. C. Formation of microscopic voids in resin transfer molded composites. *J. of Engineering Materials and Technology.* vol. 126(4), pp. 420-426. (2004) <https://doi.org/10.1115/1.1789958>
11. Hu, Q., Gumerov, N.A., Duraiswami, R. Scalable fast multipole methods on distributed heterogeneous architectures. *Proc. Supercomputing'11, Seattle, Washington* (2011) <https://doi.org/10.1145/2063384.2063432>
12. Hu, Q., Gumerov, N.A., Duraiswami, R. Scalable Distributed Fast Multipole Methods. *Proc. 2012 IEEE 14th International Conference on High Performance Computing and Communications, UK, Liverpool*, pp. 270-279 (2012) <https://doi.org/10.1109/ipdpsw.2014.110>
13. Itkulova (Pityuk) Yu.A., Abramova O.A., Gumerov N.A. Boundary element simulations of compressible bubble dynamics in Stokes flow. *ASME 2013. IMECE2013-63200, P. V07BT08A010.* (2013) <https://doi.org/10.1115/imece2013-63200>
14. Itkulova (Pityuk) Yu.A., Abramova O.A., Gumerov N.A., Akhatov I.S. Boundary element simulations of free and forced bubble oscillations in potential flow. *Proceedings of the ASME2014 International Mechanical Engineering Congress and Exposition.* vol 7. IMECE2014-36972 (2014). <https://doi.org/10.1115/IMECE2014-36972>
15. LeBel F., Fanaei A.E., Ruiz E. and Trochu F. Prediction of optimal flow front velocity to minimize void formation in dual scale fibrous reinforcements. *Int J Material Forming.* vol. 7(1). pp. 93-116 (2014). <https://doi.org/10.1007/s12289-012-1111-x>
16. Michaud, V. A review of Non-saturated Resin Flow in Liquid Composite Moulding processes. *Transp Porous Med.* vol. 115. pp. 581-601 (2016) <https://doi.org/10.1007/s11242-016-0629-7>
17. Pozrikidis, C. *Boundary Integral and Singularity Methods for Linearized Viscous Flow.* Cambridge University Press, Cambridge, MA., 259 p. (1992) <https://doi.org/10.1017/cbo9780511624124>
18. Saad Y. *Iterative Methods for Sparse Linear System.* 2nd. ed. Philadelphia: SIAM. 534 p. (2000) <https://doi.org/10.1137/1.9780898718003>
19. Sangani, A.S., Mo, G. An  $O(N)$  algorithm for Stokes and Laplace interactions of particles. *Phys. Fluids.* vol. 8(8), pp. 1990-2010 (1996) <https://doi.org/10.1063/1.869003>
20. Tan H. and Pillai K.M. Multiscale modeling of unsaturated flow in dual-scale fiber preforms of liquid composite molding I: Isothermal flows. *Composites Part a-Applied Science and Manufacturing.* vol. 43(1). pp. 1-13 (2012). <https://doi.org/10.1016/j.compositesa.2010.12.013>
21. Tornberg, A.K., Greengard, L. A fast multipole method for the three-dimensional Stokes equations. *J. Comput. Phys.* 227(3), pp. 1613-1619 (2008) <https://doi.org/10.1016/j.jcp.2007.06.029>
22. Zinchenko, A.Z., Davis, R.H. A multipole-accelerated algorithm for close interaction of slightly deformable drops. *J. Comp. Phys.* vol. 207. pp. 695-735 (2005) <https://doi.org/10.1016/j.jcp.2005.01.026>
23. Zinchenko, A.Z., Rother, M.A., Davis, R.H. A novel boundary-integral algorithm for viscous interaction of deformable drops. *Phys. Fluids.* vol. 9(6), pp. 1493-1511 (1997) <https://doi.org/10.1063/1.869275>